# PM2.5 exposure differences between children and adults

Lorenz Harr [a,*], Tim Sinsel [a], Helge Simon [a], Oliver Konter [a], Damian Dreiseitl [a],
Philipp Schulz [a], Jan Esper [a,b]

[a] *Department of Geography, Johannes Gutenberg-University, Johann-Joachim-Becher-Weg 21, 55128 Mainz, Germany*
[b] *Global Change Research Institute of the Czech Academy of Sciences (CzechGlobe), 60300 Brno, Czech Republic*

ARTICLE INFO

ABSTRACT

Heights of children and adults vary substantially and may cause different exposure to $PM_{2.5}$ particles. We measured pedestrian $PM_{2.5}$ exposure by foot following a 5.5 km route along kindergartens and schools in Mainz (Germany). Measurements were conducted in November 2019 on eight consecutive days at two heights, the potential breathing heights of adults in 1.6 and children in 1.0 m using Alphasense OPC-N3 low-cost sensors. We found that regardless of height level, persisting calm weather conditions including low wind speeds $<1.0$ m/s and lack of precipitation lead to increased $PM_{2.5}$ exposure exceeding 67.8 µg/m$^3$. Comparing the height levels revealed that the children were exposed to $>20\%$ higher concentrations on six days ($p < 0.01$), on a single day this difference exceeded 80% (24.7 µg/m$^3$). Differences generally increased with increasing $PM_{2.5}$ concentrations, though the latter are largely independent of the position along the route but varied strongly among days. These findings are supported by a microclimate simulation including traffic exhaust emissions revealing strongest height differences nearby streets with high traffic intensities. Our results demonstrate that children are exposed to considerably higher levels of $PM_{2.5}$ that are typically not observed in the stationary networks recording aerosols on only one level.

## 1. Introduction

Various epidemiological studies provide evidence that air pollution exposure has negative effects on public health causing respiratory and cardiovascular diseases and even increase mortality (Feng et al., 2016; Lelieveld et al., 2019). Fine particles with a size $<2.5$ µm can reach the lungs via the respiratory tract and cause airway inflammation followed by a decrease in lung function and even chronic obstructive pulmonary disease (Gualtieri et al., 2011; Lelieveld et al., 2019; Torres-Ramos et al., 2011).

Children are particularly exposed to ambient particulate matter. As they breathe more air per body size and have a greater risk due to their smaller airways than adults (Goldman, 1995; Mazur, 2003). Their respiratory system is not completely developed, they are exposed to an increased risk of developing respiratory diseases and exacerbation of asthma (Habre et al., 2014; Nachman and Parker, 2012).

In urban environments, $PM_{2.5}$ concentration largely stems from locally emitted sources including traffic related particles (exhausts, tyre and break abrasion), house heating, construction sites, soil and biogenic compositions (Azarmi et al., 2016; Karagulian et al., 2019; Kumar et al., 2015). Factors influencing ambient concentrations include the number of emitters as well as mesoscale weather

---

* Corresponding author.
  *E-mail address:* L.Harr@geo.uni-mainz.de (L. Harr).

condition. Anticyclonic weather in European autumn and winter is characterized by low wind speeds and little to no precipitation (Czernecki et al., 2017; Graham et al., 2020). Mesoscale high pressure systems lower atmospheric mixing layer heights (MLH) hindering vertical dispersion of air pollutants, which in turn causes an accumulation of locally emitted $PM_{2.5}$ within the planetary boundary layer (Tang et al., 2016; Wagner and Schäfer, 2017).

Several studies found that pollutant concentration decreases with increasing height above ground (Goel and Kumar, 2016; Imhof et al., 2005; Kumar et al., 2008; Zauli Sajani et al., 2018; Zhou et al., 2019). However, only a few studies examined vertical differences near the surface in heights <2 m (Garcia-Algar et al., 2015; Goel and Kumar, 2016; Kumar et al., 2017; Sharma and Kumar, 2020), whereby these are particularly important when it comes to pedestrian exposure. The smaller size of children in comparison to adults means their breath levels are closer to pollutants emitted near ground, making them potentially more vulnerable to emissions by traffic-related exhausts and whirled up fine particles (Kumar et al., 2017; Sharma and Kumar, 2020).

To examine potentially varying exposure differences between adults and children, we measured $PM_{2.5}$ at two heights, 1.0 m and 1.6 m, in a dense urban environment featuring different traffic intensities. The measurements were conducted using self-designed monitoring systems hosting Alphasense OPC-N3 low-cost sensors (Alphasense, 2018). The sensors are easily portable due to their small size and weight, and perform well under laboratory conditions (Morawska, 2018; Sousan et al., 2016), making them suitable for studies about spatial particulate matter exposure (Brattich et al., 2020; Bulot et al 2019). However, under ambient air conditions in urban areas, the accuracy of measurements is negatively affected by changing particle compositions and even more so by changing relative humidity (Alfano et al., 2020; Brattich et al., 2020; Crilley et al., 2018; Di Antonio et al., 2018). These limitations were addressed by calibrating the sensors and comparing the empirical findings with simulations from a microscale model considering particle advection and dispersion modelling was conducted (Singh et al., 2003).

The main objective of this study is to examine potential differences of $PM_{2.5}$ exposure between children and adults in an urban area at high spatiotemporal resolution. We (i) compare changes in $PM_{2.5}$ concentrations related to changing weather conditions, (ii) quantify the absolute and relative exposure differences between children and adults considering the position on the measurement route, and (iii) assess findings by comparing measured differences with microclimate simulation outputs.

## 2. Material and methods

### 2.1. Study characteristics

The study was conducted in Mainz-Neustadt, an urban area district of Mainz, the capital of Rhineland-Palatinate in South-West Germany (50.0°N, 8.26°E, Fig. 1a). Mainz is an inland city with approximately 220,000 inhabitants, located in a landscape of gently rolling hills to the west of the Rhine river. The climate is temperate with an annual average temperature of 10.7 °C and precipitation of 620 mm (Koeppen Cfb). The winters are cool and dry. From November to March, the mean air temperature is 3.9 °C and mean precipitation is 48 mm (Deutscher Wetterdienst, 2021a, 2021b). The urban architecture of this densely populated area consists of compact midrise structures with a grid-based street layout (Stewart and Oke, 2012). The streets are mostly narrow (10 m wide) and feature low traffic intensity. The city quarter is surrounded by larger multi-lane roads with high traffic volume.
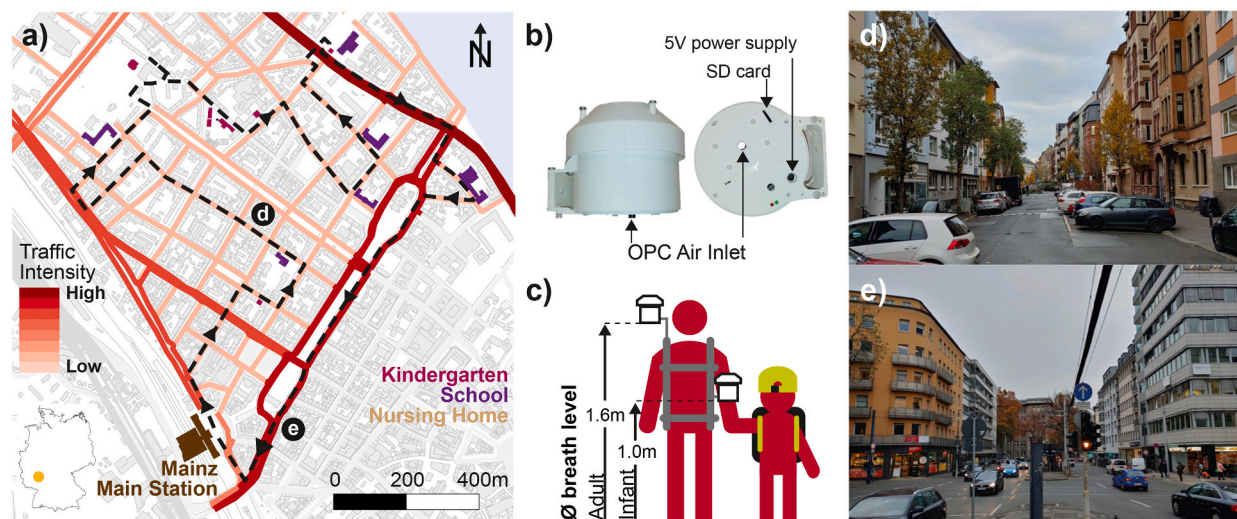


**Fig. 1.** Location of the study district Mainz-Neustadt including the start/end point Mainz main station (brown) of the measurement transect (dashed black line) with nearby social institutions, i.e., kindergartens (pink), primary and secondary schools (purple) and nursing homes (light brown). The streets within the district are colored depending on traffic intensity **a**. Design of the measurement devices (dimensions: 11.5 cm × 14 cm × 12.5 cm) **b**. Two devices mounted offset on the front of a wearable rack at breath levels of adults (1.6 m) and children (1.0 m), respectively **c**. Typical city block street canyons with low **d** and high traffic intensity **e**.

To capture local differences in PM$_{2.5}$ concentration, a clockwise circular, 5.5 km-long measurement track passes through both, the inner narrower low traffic parts as well as the larger roads of the Neustadt (Fig. 1 a). The track starts at Mainz Main Station (50.0017°N, 8.2595°E), then runs within the inner part of the district, passing social institutions, i.e., kindergartens, primary and secondary schools as well as nursing and retirement homes. After leaving the center of the quarter, the transect continues along roads with high intensity of traffic, first in southeast, then in southwest direction (Fig. 1 e) ending at the Main Station.

The measurement campaign took place from 11 to 20-2019 to 11-27-2019 (Wednesday to Wednesday). The measurement runs were conducted by foot starting at 3:15 pm and ending at ~4.30 pm every day covering the time of daily of kindergarten and school endings and start of the rush hour within the study area. For each run, two devices containing a PM sensor (Alphasense, 2018), a GPS module (Simcom, 2021), a ESP32 as microcontroller (Espressif, 2021) and a microSD card for saving the data were used (Fig. 1b). The cover of the cases protruded all around over the side parts were similar to a radiation shield cap to support an unconstrained outflow of the air sample. The devices were mounted at the breath level of adults (1.6 m, device A) and children (1.0 m, device B). To reduce influences induced by the measuring person, the devices were attached at the front of the body at a distance of 30 cm (Fig. 1 c). Every run was filmed with a camera to facilitate detections of possible local emitters in the postprocessing of the measuring campaign.

## 2.2. Meteorological data

A detailed description of the meteorology during the measurement period is needed as the local weather characteristics affect the type, number, and duration of particulate matter concentrations (Cheng and Li, 2010; Graham et al., 2020; McGregor and Bamzelis, 1995). The central emission network of Rhineland-Palatinate kindly provided 3-min-arithmetic-means of air temperature, relative humidity, precipitation, and atmospheric pressure (Fig. S1), measured at the station Mainz-Zitadelle (49.9950°N, 8.2739°E) located ~1.2 km west of the study area, as well as 3-min-sums of precipitation, wind direction and speed at the station Mainz-Mombach (50.0180°N, 8.2157°E) located ~3 km west of the study area (ZIMEN, 2019). Data of the convective inhibition energy (CIN) and mixing-layer height (MLH), indicators for the stability of the air near the ground, were measured with a radiometer located ~500 m west of the study area (50.01406°N 8.257°E). These data were provided by the environmental meteorology unit of the environmental state office of Rhineland-Palatinate (Umweltmeteorologie RLP, 2019).

## 2.3. Calibration of PM$_{2.5}$ sensors

The PM$_{2.5}$ measurements on both breathing heights were conducted using an Alphasense OPC-N3 sensor (Alphasense, 2018). The OPC-N3 is a low-cost optical particle counter using the light scattering principle to count particles (Mie, 1908). The total number counted is processed internally in the sensor, categorized by estimated particle size in 24 classes using software bins (Alphasense, 2018; Bohren and Huffman, 1998) and converts the data into mass concentrations (Walser et al., 2017). During the default settings of the sensor's principles were made.

Both OPC-N3 sensors were manufacture-calibrated following the European Standard EN 481 (Crilley et al., 2018). However, to improve sensor accuracy, a field calibration in an environment comparable to the study area has been conducted (Alfano et al., 2020;



**Polynomial regression formulas**
$f(x) = 5.93 \cdot 10^{-6} \cdot x^4 - 7.35 \cdot 10^{-4} \cdot x^3 + 2.41 \cdot 10^{-2} \cdot x^2 + 0.86 \cdot x + 0.36$
$g(x) = 8.18 \cdot 10^{-6} \cdot x^4 - 1.25 \cdot 10^{-3} \cdot x^3 + 5.83 \cdot 10^{-2} \cdot x^2 + 0.65 \cdot x + 0.76$

RH [> 85] [%]
$R^2 = 0.94$
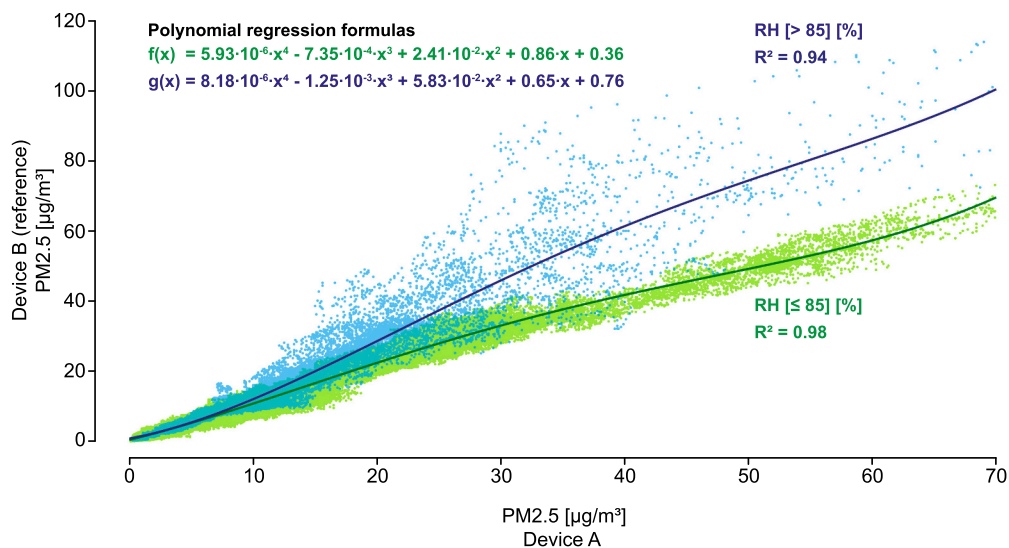
RH [≤ 85] [%]
$R^2 = 0.98$

**Fig. 2.** Scatter plots and polynomial regression curves of devices A and B PM2.5 measurements from the adjustment period 12-22-2019 to 12–31–2019. The green data and curve show the measurements for RH ≤ 85% and the blue data for RH > 85% (blue dots and line), as well as the regression equations and coefficients $R^2$, respectively.

Chatzidiakou et al., 2019; Crilley et al., 2020; Gysel et al., 2007; Hagler et al., 2018). This was done from 12 to 22-2019 to 12-31-2019 at the official measurement station Mainz-Zitadelle (49.9950°N, 8.2739°E) of ZIMEN. Both Alphasense devices were located side-by-side on the same height measuring PM2.5-concentration at a 1 s interval. The data were then transformed into running 20 s-truncated arithmetic means and humidity-corrected to mitigate the influence of fine particle hygroscopy (Crilley et al., 2018; Petters and Kreidenweis, 2007). The correction is based on the $k$-Köhler-theory considering a particle hygroscopy of $k = 0.33$, density of particles of 1.65 g/cm$^3$ (Crilley et al., 2020), and ambient relative humidity recorded at the official station Mainz-Zitadelle.

The scatter plot between $PM_{2.5}$ data from devices A and B reveal high precision measurements when RH ≤ 85% as reflected by the explained variance ($R^2 = 0.98$) and data homoscedasticity (Fig. 2). This allowed a reliable comparison of $PM_{2.5}$ measurements by transforming the measurements of device A considering the 4th degree polynomial regression model shown as a green curve in Fig. 2. For the data recorded at RH > 85%, the PM2.5 correlation and resulting correction are weaker (blue data, Fig. 2). The scatter plot includes an obvious heteroscedasticity for $PM_{2.5} > 10$ μg/m$^3$ largely driven by increased residuals in device A $PM_{2.5}$-concentrations. This increased variability of OPC-N3 devices is in line with results by Brattich et al., 2020 revealing similar biases for the predecessor device, OPC-N2, and identifying a systematic misclassification of particulate matter sizes during high relative humidity conditions. These results question the reliability of $PM_{2.5}$ data recorded at RH > 85%. Nevertheless, these measurements are fitted with a different model, shown as the blue curve in Fig. 2, considering the weak reliability for $PM_{2.5} > 10$ μg/m$^3$.

## 2.4. Postprocessing analysis

After each measurement run, several postprocessing steps were carried out to support the comparison between heights and among runs. The datasets of devices A and B were adjusted by time (Wickham, 2020), the $PM_{2.5}$-concentrations, recorded in a 1 s-interval, transformed into a running 20 s-truncated arithmetic mean, and the 10% highest values removed to mitigate the influence of local short-term emissions (e.g. smokers or street cleaning). Since the duration of the different runs varied slightly and minor inaccuracies affected the recorded GPS data, an additional synchronizing procedure was applied: We calculated a mean standard route considering a concave hull surrounding all runs and retrieving the mean by the skeleton algorithm of the GRASS GIS Processing Toolbox (Fortune, 1987; McCauley et al., 2020). A few remaining inaccuracies were re-digitized manually. The standard route was converted to points with a distance of 20 cm to each other (total $n = 27,515$). Each point was assigned the appropriate $PM_{2.5}$-concentration, in which all values within a search radius of 15 m are averaged using an inverse distance weighting method (Shepard, 1968). If less than 10 measurements were found, the radius was increased to 50 m.

The $PM_{2.5}$ data were adjusted using the same humidity correction method as during the calibration (Crilley et al., 2018; Crilley et al., 2020). To compare absolute $PM_{2.5}$ values, device A data were transformed considering the regression equation from a polynomial fit against the device B data (Fig. 2).

The adjusted $PM_{2.5}$ data were analyzed using descriptive statistics, i.e., arithmetic mean, median, standard deviation (SD), and coefficient of variation (CV). Cubic smoothing splines (degrees of freedom = 55, n = 27,515) were calculated to reduce the sensitivity of $PM_{2.5}$ measurements to short-term extreme concentrations. The correlation coefficient R was used to quantify the relation between the measurements of the two heights and respective smoothing splines. To assess differences between 1.0 m and 1.6 m levels, the root-mean-square error (RMSE) was calculated considering daily data, and residuals and relative differences were calculated in cases of pronounced differences in PM2.5-concentrations. Welch's $t$-test was conducted to assess statistically significant differences in case of unequal variances.

## 2.5. Simulation setup

To examine whether traffic exhausts can be assigned as a cause for varying particulate matter exposures along streets with high traffic intensities, a pollutant dispersion simulation for one exemplary day of the measurement period was conducted. This simulation was performed using the holistic ENVI-met microclimate model, which is able to simulate pollutant concentration distributions for specific meteorological conditions in complex urban environments (Bruse, 1999; Nachman and Parker, 2012; Wania et al., 2012).

The 11-24 was selected as is represents a day of average meteorological conditions and $PM_{2.5}$ concentrations after a short period of

**Table 1**
Model parameters of the simulated emissions for 11-24-2019 in ENVI-met.

| | |
|---|---|
| Start date and time (Local) | 11-24-2019 11:00 |
| Duration [h] | 10 |
| Wind Speed [m/ s] | 1.0 |
| Wind Direction [°] | 115 |
| Meteorological Boundary Conditions | Full Forcing |
| Emission height [m] | 0.2 |
| Location Lat (Lower Left Corner) | 50.01°N |
| Location Lon (Lower Left Corner) | 8.25°E |
| Dimensions | 280 × 250 × 26 |
| Resolutions (X, Y, Z) [m] | 5 × 5 × 2 |
| Lowest Grid Cell Splitted | Yes |
| Telescoping: Factor & Starting Height | 30% above 28 m |
| Height of 3D Model Domain [m] | 221 |

air mass exchange the day before. RH was <85% during the time of the run, so the measurements should be reliable (Fig. S1). The modelled area covers the district of Mainz-Neustadt with a dimension of 280 × 250 × 26 grids at 5 × 5 × 2 m per grid (Table 1). The simulation started with full forcing at 11 am using the 30 min mean-meteorological parameters of that day as meteorological boundary conditions (Fig. S1). Wind speed and direction were set constant to avoid instabilities in the model. Radiation was forced by only cloud coverage as measured values were not available.

The applied PM2.5 emissions originating from vehicle exhausts were implemented as source emission profiles at a height of 20 cm in the model. The diurnal profiles of traffic exhaust emissions are based on the handbook of emission factors for Road Transport (Environmental Protection Agency of Germany (UBA), 2017) and the amounts of emitted $PM_{2.5}$ in the model area were related to the intensity of traffic per lane (Fig. 1). Detailed settings about the traffic emission profiles are described in Simon et al. (2019), where model area and traffic intensities were initially used. The relative differences of PM2.5 concentrations were computed between 1.0 m and 1.8 m due to the simulations grid cell resolution of only 0.4 m to compare the model outputs to the measurement data.

## 3. Results

### 3.1. Weather conditions

During the measurement period, the weather situation was dominated by a continental anticyclone centered over Eastern Europe, ~ 2000 km away. On 11-20 and 11-22, Germany was located between a long wave trough in the west and a ridge in the east. This led to weak atmospheric pressure gradients (~Δ 10 hPa around 1003 hPa) and calm weather characterized by low wind speeds (<0.8 m/s), small daily temperature gradients (max. Δ 5.3 °C, 1.6 °C – 6.9 °C on 11-22) and relative humidity ranging from 72 to 90%. CIN was subjected to diurnal courses with increasing gradients (Δ 106 J/kg around 89 J/kg to Δ 163 J/kg around 181 J/kg) which led to lower maximum MLH, declining from 386 to 300 m a.g.l., and low stratus conditions in Mainz (Hoffmann, 2019; Table 3). Starting on 11-22 ~ 2:30 pm, the anticyclonic influence was interrupted by weak cyclonal conditions, which led to a dissolution of low stratus in Mainz in the morning of 11-23 (Zeuschner, 2019). Wind speed rose to 1.6 m/s at 11 am, interrupted by an absence of wind at around 2:30 am. The atmospheric pressure gradient decreased slowly reaching a minimum of 982 hPa in the afternoon and TA increased up to 11.7 °C. However, the CIN gradient decreased (Δ83 J/kg 177 J/kg) but remained >100 J/kg indicating that, at the end of 11-23, the ridge of the anticyclone became influential again. Starting on 11-24, the wind speed declined <0.5 m/s and temperatures and the air pressure increased to maxima of 9.8 °C and 999 hPa, respectively. Moreover, relative humidity rose to a maximum of 92.2% in the morning of 11-25 and remained > 83.5% thereafter. On 11-26, the weather changed from an anticyclonic to a calm cyclonic situation characterized by a slowly decreasing air pressure from 999 to 990 hPa, rising temperatures to 11.4 °C, and low wind speeds <0.5 m/s. However, on 11-27, the last day of the study, wind speed increased again to a maximum of 1.1 m/s, while temperatures still increased (to 12.3 °C) and precipitation started, summing up to 13.4 mm. The influence of the anticyclone on the weather situation thus retreated.
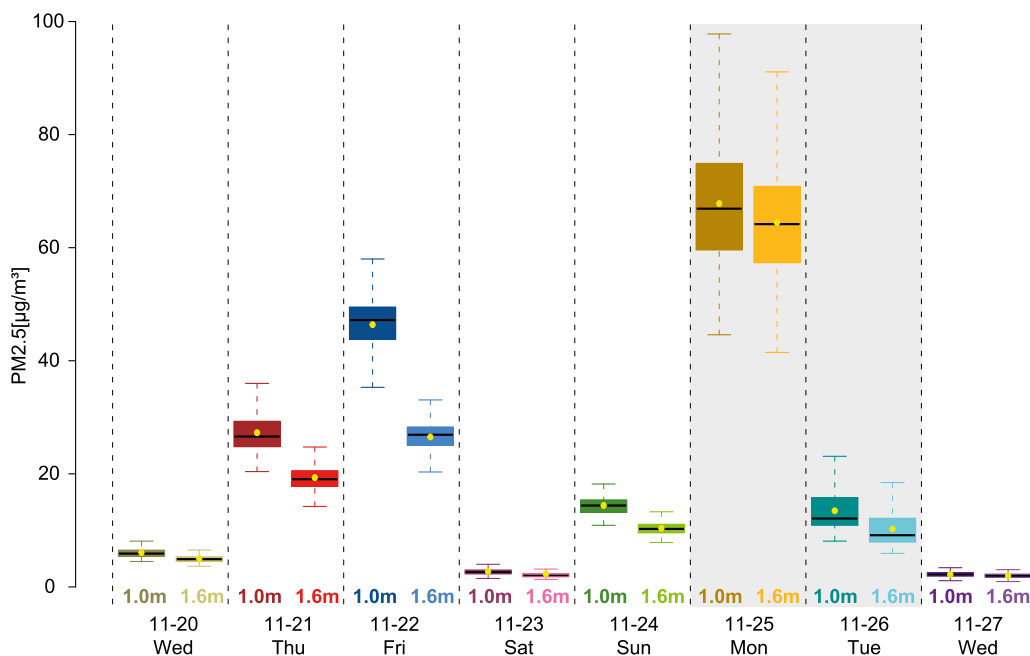


**Fig. 3.** PM$_{2.5}$-concentrations at the 1.0 and 1.6 m levels for every run from 11 to 20 to 11-27 visualized as boxplots with whiskers (length 1.5 * interquartile range), median (black bar) and mean (yellow dot). Grey background indicates RH > 85% during the run.

**Table 2**

PM$_{2.5}$ characteristics at 1.0 m (dark yellow) and 1.6 m (light yellow) for the 8-day measurement campaign. SD is standard deviation, CV is coefficient of variation.

| Date | 11-20 | | 11-21 | | 11-22 | | 11-23 | | 11-24 | | 11-25 | | 11-26 | | 11-27 | |
|---|---|---|---|---|---|---|---|---|---|---|---|---|---|---|---|---|
| Mean PM2.5 [μg/m$^3$] | 6.1 | 5.0 | 27.3 | 19.3 | 46.4 | 26.5 | 2.7 | 2.3 | 14.4 | 10.4 | 67.8 | 64.4 | 13.5 | 10.2 | 2.2 | 2.0 |
| Median PM2.5 [μg/m$^3$] | 5.9 | 4.9 | 26.6 | 19.1 | 47.3 | 26.9 | 2.6 | 2.0 | 14.4 | 10.3 | 66.9 | 64.2 | 12.1 | 9.1 | 2.2 | 2.0 |
| SD [μg/m$^3$] | 1.2 | 1.1 | 3.6 | 2.4 | 4.7 | 2.4 | 0.9 | 1.4 | 1.4 | 1.1 | 10.6 | 9.9 | 3.8 | 3.3 | 0.5 | 0.4 |
| CV | 0.19 | 0.21 | 0.13 | 0.12 | 0.10 | 0.10 | 0.33 | 0.61 | 0.10 | 0.10 | 0.16 | 0.15 | 0.28 | 0.32 | 0.22 | 0.20 |
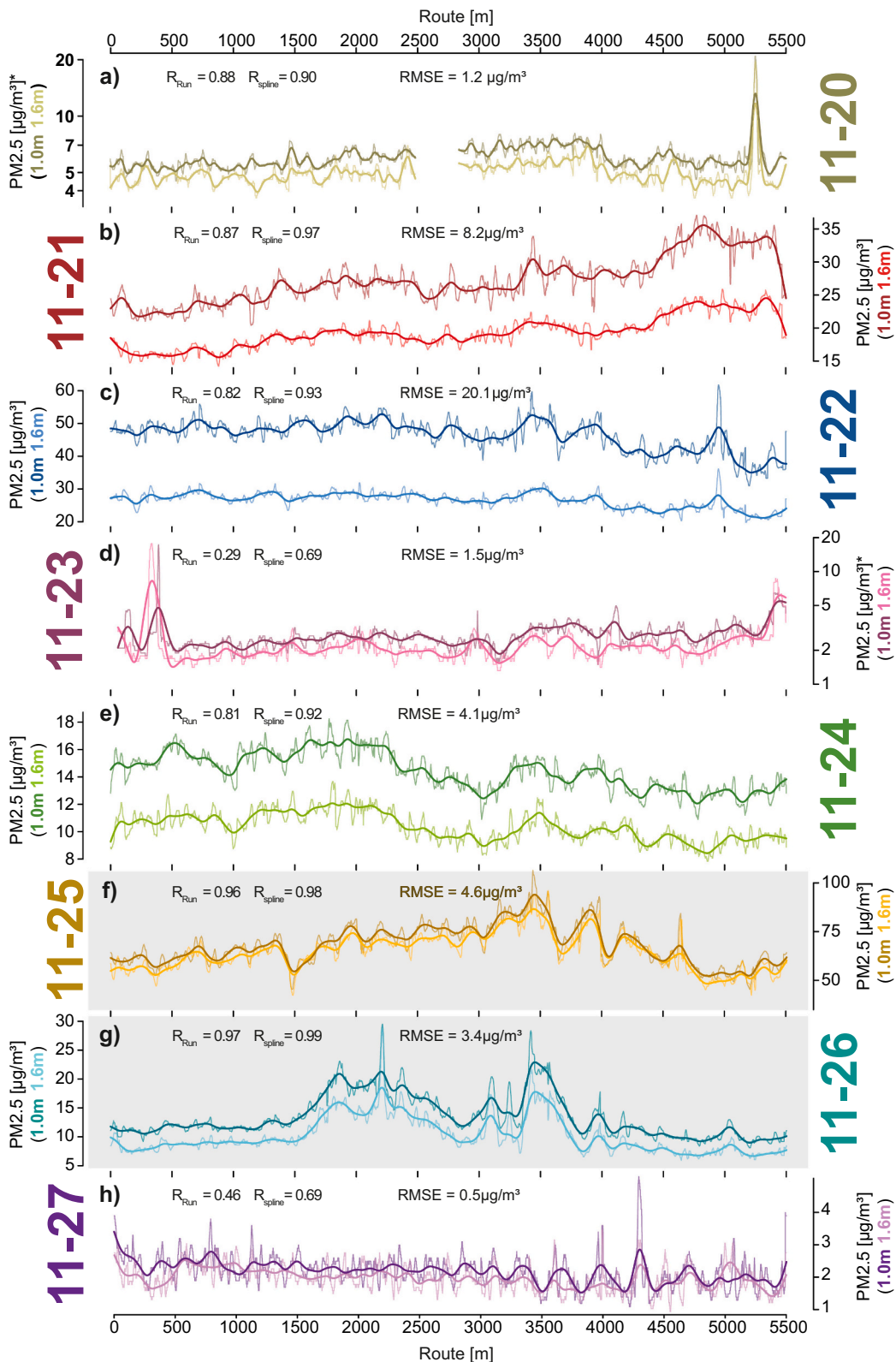
**Fig. 4.** Distribution of 20 s PM$_{2.5}$ concentrations at 1.0 m (dark curves) and 1.6 m level (bright curves) on days 11-20 (**a**) to 11-27 (**h**) along the route. Bold curves are smoothing splines (df = 55, *n* = 27,515) and grey background indicates runs with RH > 85%. *Logarithmic y-axis used in panel **a** and **d**.

## 3.2. Recorded PM$_{2.5}$ concentrations

Fig. 3 shows the PM2.5-concentrations at the 1.0 and 1.6 m levels for every run of the measurement campaign. The absolute PM2.5 concentrations at both levels differed substantially among runs over the course of the period from 11 to 20 to 11-27. Mean PM2.5-concentrations at 1.0 m increased from 6.1 µg/m$^3$ on 11-20 to 46.4 µg/m$^3$ on 11-22, then declined massively to 2.7 µg/m$^3$ on 11-23, reached a distinct peak of 67.8 µg/m$^3$ on the next day and then decreased to 2.2 µg/m$^3$ until 11-27 (Table 2).

During all days, the PM$_{2.5}$-concentrations at 1.0 m were higher than on 1.6 m (Table 2). On 11-20, 11-21, 11-22 and 11-24 the interquartile ranges (IQR) do not overlap, indicating that at least 75% of the PM$_{2.5}$ concentrations measured at 1.6 m are lower than at least 75% of the PM$_{2.5}$ values at 1.0 m. The temporal distribution along the days (Fig. 4) shows that on 11-21, 11-22 and 11-24 the concentrations at the children breath level were constantly higher than at adult level (RMSE: 8.2 µg/m$^3$, 20.1 µg/m$^3$, 4.1 µg/m$^3$, respectively).This is also the case for the run on 11-26 (RMSE: 3.4 µg/m$^3$), but the data had to be adjusted using the equation for RH > 85% (Fig. 2; Table 3).

On 11-20 and 11-23, the 1.0 m PM$_{2.5}$ concentrations were higher in 97% and 88% of all measurement points, independent of the position of the route (RMSE: 1.2 µg/m$^3$, 1.5 µg/m$^3$, respectively). For the remaining six days, the PM$_{2.5}$ concentrations were significantly higher at 1.0 m than at 1.6 m according to a Welch t-test (p < 0.01).

On 11-25, the PM$_{2.5}$ concentrations measured by device A were adjusted using the equation for RH > 85% (Fig. 2, Table 3). Considering the unexplained variance of the adjustment procedure (6%) as well as the uncertainties for PM$_{2.5}$ > 10 µg/m$^3$, the recorded differences between children and adult breathing heights were insignificant on that day. On 11-27, the differences were not distinguishable due to low absolute PM$_{2.5}$ concentrations including 97% of measurements <3 µg/m$^3$ at 1.0 m, and 99% of measurements <3 µg/m$^3$ at 1.6 m, with the absolute differences (~ 0.2 µg/m$^3$) approaching measurement accuracy.

## 3.3. Distribution of PM$_{2.5}$ along the route

The temporal variability of PM$_{2.5}$ measurements were low (CV < 0.22) as well as the differences in variability of both heights among the runs (CV difference max. 0.04; Table 2). Exceptions are the runs on 11-23 and 11-26: the high CVs (1.0 m: 0.33; 1.6 m: 0.61) on 11-23 were affected by an oncoming person at the beginning of the run, holding a cigarette between 1.0 and 1.6 m, so the devices recorded the short-term pollution shortly one after the other. The higher variabilities on 11-26 (1.0 m: 0.28; 1.6 m: 0.32) could not be attributed to single incidents, explanations could be RH > 85% as well as weakening of anticyclonic weather.

The distribution of the absolute PM$_{2.5}$ concentrations indicated common concentration patterns between the two measurement heights (R$_{Run\_all}$ > 0.8) (Fig. 4). This coherence was reduced on days with low PM$_{2.5}$ concentrations, on 11-23 and 11-27, with R$_{Run}$ = 0.29 and R$_{Run}$ = 0.46, respectively, when random variability near the measurement accuracy adds uncertainty to the data. However, there is no common temporal pattern among the runs, as some timeseries increase throughout the run (11-21), whereas other decrease (11-22) or show no long-term trend (11-27).

On 11-20 and 11-22, the differences between 1.0 and 1.6 m decline towards the end of the runs, whereas short-term PM2.5 peaks are recorded on 11-20 at ~5250 m, 11-23 at ~350 m and ~5400–5500 m, and 11-27 at ~4300 m (Fig. 4). The causes for these peaks differ though, and may include ventilation of a cellar bar (11-20), a smoking person and exceptional high traffic at the main station (11-23), or were simply not detectable (11-27). There are two distinct deviations including mean PM2.5 > 10 µg/m$^3$ detectable in all runs, however. These are located at the 'Grüne Brücke', a bridge crossing the 'Rheinallee' (Fig. 4 at 3300–3500 m; Fig. 7/8 dot 3) and the 'Rheinallee' close to the crossroad 'Rheinallee/Kaiserstraße' (Fig. 4/6 at 3800–4000 m; Fig. 7/8 dot 4).

The described trends in absolute PM$_{2.5}$ concentration among the runs change considerably when focusing on the absolute height differences between devices A and B (Fig. 5). The common PM$_{2.5}$ patterns of both measurement heights lead to the fact that the differences between top and bottom remain almost the same and thus strong deviations are largely leveled out. Only the mentioned deviations at the 'Grüne Brücke' and 'Rheinallee' were visible on 11-21, 11-22, 11-24 and 11-26.

The PM$_{2.5}$ residuals persist on most days, except of 11-25 and 11-27 due to indistinguishable differences. However, the residuals differ among the days. The amount and variability of the absolute differences seem to be depended on the level of their absolute value. The higher the particulate matter concentration was, the higher were the residuals and their absolute variability within a run. Only for 11-24 and 11-26 this hypothesis does not apply: The residual IQR of the run at 11-26 (1.0 µg/m$^3$) were slightly larger than the IQR of

**Table 3**

Meteorological conditions during the measurement campaign from 11 to 20 to 11-27 including Mean Air temperature (TA) [°C], Mean Relative Humidity (RH) [%], Precipitation Sum [mm], Atmospheric Pressure [hPA], Wind Speed [m/s], Wind Direction [°], Mean Convective Inhibition [J/kg] and Mean Mixing Layer Height [m] (Umweltmeteorologie RLP, 2019; ZIMEN, 2019).

| Date | 11-20 | 11-21 | 11-22 | 11-23 | 11-24 | 11-25 | 11-26 | 11-27 |
|---|---|---|---|---|---|---|---|---|
| TA [°C] | 5.0 | 5.9 | 6.6 | 11.5 | 8.9 | 6.7 | 11.1 | 12.3 |
| RH [%] | 77.3 | 78.1 | 81 | 62.5 | 78 | 87 | 86 | 78 |
| Precipitation [mm] | 0 | 0.1 | 0 | 0 | 0 | 0 | 0 | 4.3 |
| Atmospheric pressure [hPA] | 1004 | 998 | 996 | 987 | 997 | 999 | 994 | 983 |
| Wind direction [°] | 116 | 152 | 119 | 90 | 142 | – | – | 129 |
| Wind speed[m/s] | 0.4 | 0.1 | 0.7 | 0.5 | 0.1 | 0 | 0 | 0.5 |
| CIN [J/kg] | 62 | 134 | 113 | 156 | 164 | 149 | 100 | 88 |
| MLH [m] | 289 | 239 | 301 | 130 | 116 | 183 | 74 | 54 |
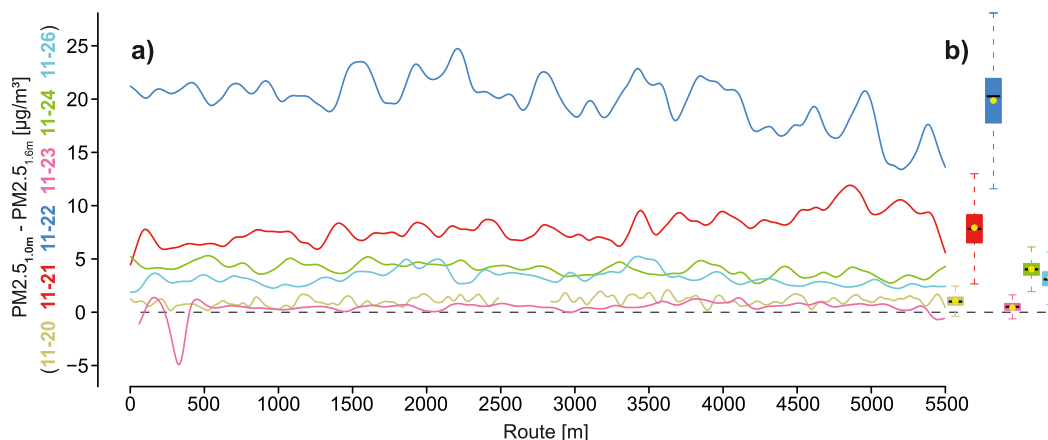
**Fig. 5.** Residuals of PM$_{2.5}$ concentrations between 1.0 and 1.6 m for days of significant PM2.5 height differences shown as smoothed deviations from 20 s PM$_{2.5}$ concentrations along the route (df = 55, n = 27,515) **(a)**, and boxplots of the data **(b)**.

the run at 11-24 (1.3 μg/m$^3$) although the 11-26 residual mean was smaller (3.2 μg/m$^3$).

To highlight the association between children and adult PM$_{2.5}$ exposures, splines of the relative differences between 1.0 and 1.6 m were calculated (Fig. 6). The ratios were largest on 11-22 reaching a maximum value exceeding 188%, nearly the double exposure for children. Following the residuals (Fig. 5), relative PM$_{2.5}$ differences correlate positively on the total amount of the measured PM$_{2.5}$, as is expressed by the lower ratios on 11-21 (141%), followed by 11-24 (139%), 11-26 (133%) and 11-20 (122%).

The IQR of the runs range from 11 to 16%, excluding the run at 11-23, affected by an oncoming smoking person. The relative differences of the run at 11-23 were exceptional, as the values varied massively around the 127% mean, expressed by an IQR of 29%. In contrast, the CV was lower, as this metric considers the (high) absolute mean value.

The pronounced extremes of absolute PM2.5 values at the 'Grüne Brücke' at 3300–3500 m are also seen in the height differences on 11-21, 11-22, 11-24 and 11-26. Similarly, the high absolute PM2.5 values at the 'Rheinallee' at 3800–4000 m also appear on 11-21, 11-22, 11-23, 11-24, 11-26, in the relative difference between devices A and B. Data variability during days with substantial height differences showed no trends. Only on 11-22 the ratios were slightly decreasing along the measurement route.

### 3.4. Simulated versus measured concentrations

The simulated PM$_{2.5}$ exposures for the run on 11-24 showed similar results: The relative differences of PM$_{2.5}$ exposure between 1.0 and 1.8 m were positive across the model area (Fig. 7, without shading Fig. S2). Ratios <100% could only be found at the borders of the model probably due to boundary modelling artifacts. Relative differences >110% were located on the roads with high traffic intensities (Fig. 1, e.g. Fig. 7 dot 4) and/or streets with the same direction as the wind (e.g. Fig. 7, dot 2). Following the measurement route, the simulation underestimated the measured relative differences by ~30% on average (Fig. 8). Starting with ~115% at Mainz main station, the simulated PM$_{2.5}$ exposures at 1.0 m were just <5% higher than at 1.8 m in the inner part of Mainz-Neustadt and showed
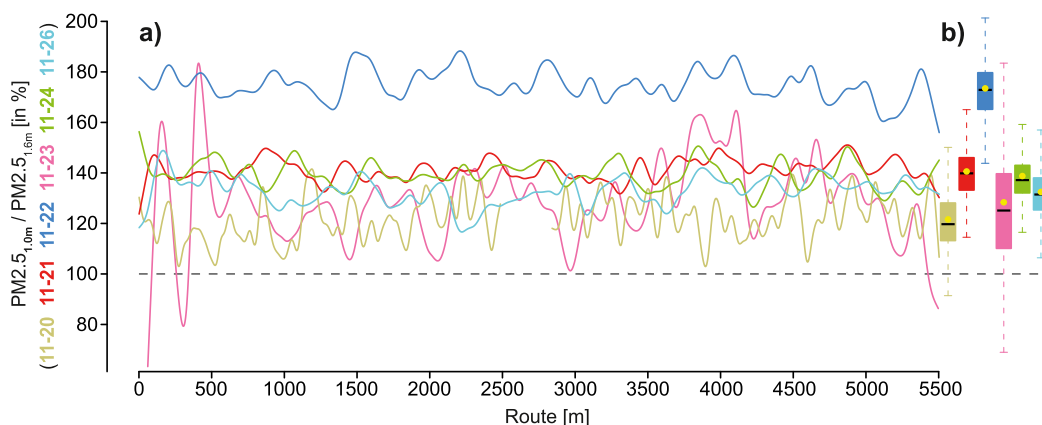


**Fig. 6.** Relative differences of PM$_{2.5}$ concentrations between 1.0 and 1.6 m for days of significant PM$_{2.5}$ height differences shown as smoothed deviations from 20 s PM$_{2.5}$ concentrations along the route (df = 55, *n* = 27,515) **(a)**, and boxplots of the data **(b)**.
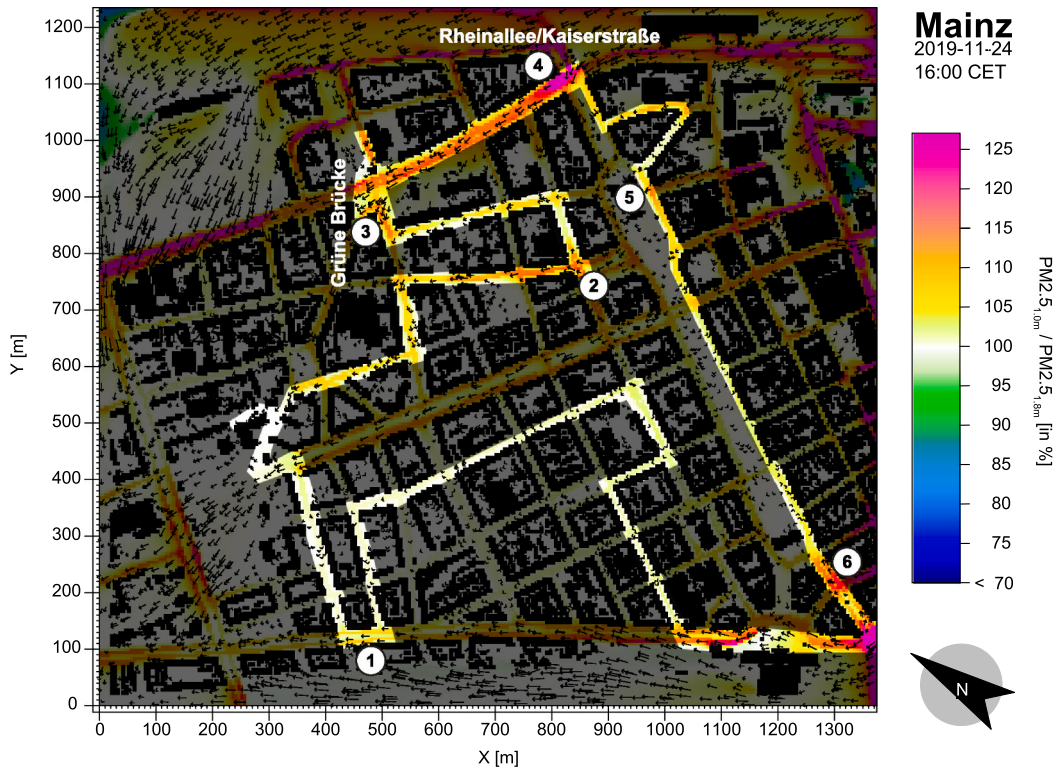
**Fig. 7.** Simulated relative differences distribution of PM$_{2.5}$ concentrations between 1.0 and 1.8 m in the study area with the measurement route highlighted. The colors display reduced (blue and green), equal (white) and increased (yellow to red/magenta) PM$_{2.5}$ exposure at 1.0 m level. The arrows represent horizontal wind speed and direction.

almost no variability in contrast to the measured PM$_{2.5}$ ratios. Areas close to streets featuring high traffic intensities showed larger relative differences of up to 127%.

Comparing the relative differences of PM$_{2.5}$ between the model and measurements along the route (Fig. 8) confirms that the model predicts both lower values and a lower variability in general. For some locations however, the model simulates similar increases in relative differences when compared to the measurements (Fig. 8, marked 1 to 6). The relative differences of the simulation increased as
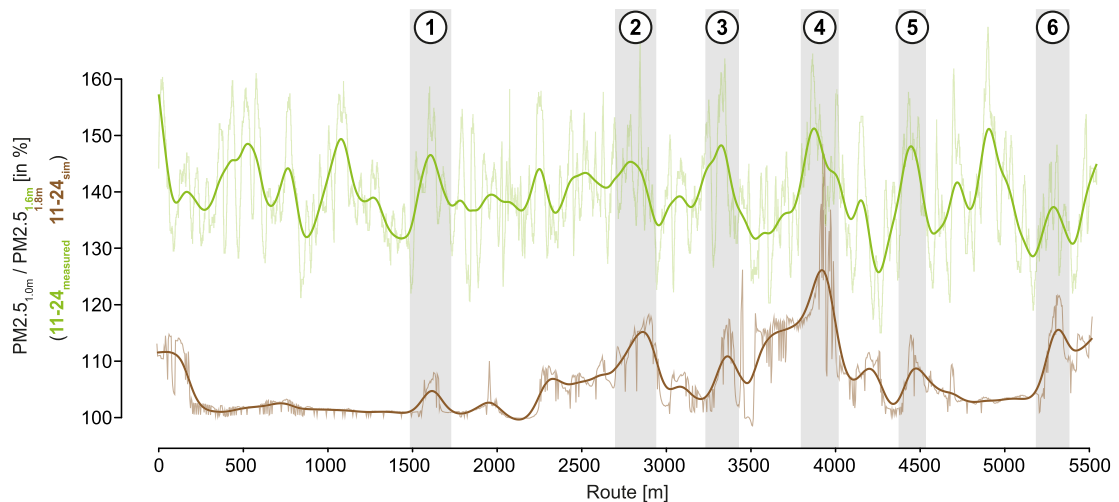


**Fig. 8.** Relative PM$_{2.5}$ exposure differences on 11-24 between 1.0 and 1.6 m as measured (green curves) and between 1.0 and 1.8 m as simulated (brown curves). Bold curves are smoothing splines (df = 55, n = 27,515).

the study route passed a street with higher traffic intensity at the western border of the district (Fig. 8, dot 1).

## 4. Discussion

### 4.1. Influence of weather conditions on PM$_{2.5}$ exposure

The continental anticyclonic conditions led to a mainly stable and calm weather throughout the study period (Fig. S2). Several studies (Cheng and Li, 2010; Czernecki et al., 2017; Graham et al., 2020; Hamburger et al., 2011) showed that the longer the stability of anticyclonic weather endured, the higher PM$_{2.5}$ concentrations increased. Our work corroborates this finding: When the weather situation was stable with low wind speeds <1 m/s and a lack of precipitation, the PM$_{2.5}$ values increased from 11 to 20 to 11-22 (Fig. 2; Table 2). From 11 to 22 to 11-23, the absolute PM$_{2.5}$ concentrations declined due to a short-term cyclonical influence with wind speeds >1 m/s. Subsequent to this exchange of air masses, anticyclonic conditions fostered PM$_{2.5}$ increases on 11-24 and 11-25, until the influence weakened due to an upcoming cyclone with higher wind speed and minor precipitation towards the end of the measurement campaign. However, the concentrations recorded in this study exceeded the European law threshold of 20 μg/m$^3$, as a benchmark for yearly mean PM$_{2.5}$ exposure (European Parliament and Council (EU), 2008), in only three of eight runs. These effects were observed at both heights, which indicates that the changes in absolute PM$_{2.5}$ concentrations throughout the week were largely weather driven.

### 4.2. Local emissions and vertical PM$_{2.5}$ differences

We showed that in six of eight runs, PM$_{2.5}$ concentrations were significantly higher at the breath level of children than of adults. The exposure is at least 41% higher, and during the calm weather conditions on 11-22, grew up to 89% (75% on average), which means that children were exposed up to 24.7 μg/m$^3$ higher PM$_{2.5}$ concentrations.

Our results are consistent with the findings of studies made by Garcia-Algar et al. (2015), Kumar et al. (2017) and Sharma and Kumar (2020). Garcia-Algar et al. (2015) conducted a study measuring ultrafine particles at the height of strollers (0.55 m) and adults (1.70 m) by foot on three randomly chosen streets with high traffic intensity 20 times on 10 consecutive days in Barcelona, Spain. They showed that the exposure is 10% higher on stroller level. Kumar et al. (2017) measured PM2.5 exposure to in-pram babies (0.7 m) and the carrying adult (1.4 and 1.6 m) also by foot 32 times on a predefined route (2.1 km) in Guilford, UK during morning (8 to 10 am) and afternoon (3 to 5 pm). They found out that in the morning hours, the infants were 5% significantly lower exposed than adults. However, in the afternoon, the concentrations were 10% significantly higher for the children. Sharma and Kumar (2020) reconducted this study in 2018 on a similar but shorter route (2.1 km) in Guildford, UK; showing that the PM2.5 concentrations at 0.7 m are up to 44% higher in the afternoon. All of these three studies concluded that traffic-related sources were major factors (Garcia-Algar et al., 2015; Kumar et al., 2017; Sharma and Kumar, 2020). We also assume that our results are affected by the prevailing calm weather during the study period. McGregor and Bamzelis (1995), for instance, showed that low wind speeds, caused by continental anticyclonic conditions, limited air mass exchange in Birmingham, UK and concluded that measured particulate matter had to be emitted locally. The local, ambient PM$_{2.5}$ in the urban area of Mainz-Neustadt are likely emitted by combustion processes, i.e. traffic and domestic heating, whirled up dust, tyre and break abrasion, as well as floating soil or biogenic compounds and deposited particulate matter (Karagulian et al., 2015). Except domestic heating, all particle sources are close to the surface. In consequence, high traffic volumes are expected to cause high particulate matter emissions near the ground. Moreover, the measurement runs (~3:15 pm to ~4:30 pm) took place during the daily afternoon rush hour, a time with higher traffic volume. The rush hour typically starts at ~3 pm with the daily end of service in the kindergartens and all-day schools but also with the end of working days within the study area. This means that parents are picking up their children, and people are commuting in the beginning rush hour traffic, thereby increasing PM$_{2.5}$ emissions. The increase of these means of mobility during the afternoon rush hour probably led to higher PM$_{2.5}$ concentrations near ground and caused larger PM$_{2.5}$ exposure for children than for adults within the study area.

Additionally, we observed that the absolute and the relative differences in PM$_{2.5}$ exposure between both levels depended on the total amount of PM$_{2.5}$. The higher the concentration of particulate matter, the higher the absolute and relative differences (Fig. 5/6). As stated before, in the case of emissions in calm weather situations with low wind speeds, PM$_{2.5}$ will remain near the ground. The absolute and relative PM$_{2.5}$ differences between 1.0 and 1.6 m increase with increasing PM$_{2.5}$ concentrations.

The absolute and relative difference between both heights were largely independent of the position on the study route. Even in areas with low traffic, the differences were at the same level as in streets with high traffic intensity. The lack of spatial variability in PM$_{2.5}$ differences is expressed by high correlations ($R > 0.8$) and similar CV of each run's measurements. Both heights had similar courses in PM$_{2.5}$ concentration, so strong deviations were leveled out after calculating differences.

There are two locations that stood out for relative and absolute PM$_{2.5}$ concentrations: 'Grüne Brücke' (Fig. 4 at 3400–3500 m; Fig. 7/8 dot 3) and 'Rheinallee' close to the crossroad 'Rheinallee/Kaiserstraße' (Fig. 4/6 at 3900–4000 m; Fig. 7/8 dot 4). The 'Grüne Brücke' is a pedestrian bridge with extensive planting crossing the 'Rheinallee', a road with high traffic intensity (Fig. 1). When the wind arrives from an easterly direction, the bridge and adjacent buildings of the 'Josefstraße' form a barrier for particles perpendicular to the 'Rheinallee' (Table 3). On days with high absolute PM$_{2.5}$ concentrations (11-21, 11-22, 11-24), the traffic-related PM$_{2.5}$ accumulated and additionally increased the height differences due to a lack of vertical air exchange. These findings corroborate with Gallagher et al. (2015) showing that surrounding buildings are solid barriers for air flow hindering particulate matter to disperse within street canyons. The second site at the 'Rheinallee' is bounded by 5-story-high blocks on two sides in north-south direction, with the northern block tapering down to the intersection 'Rheinallee/Kaiserstraße'. The intersection itself is free of buildings in the northeast direction. As a result, during easterly winds, traffic-related particles are pushed into the 'Rheinallee' and accumulate behind

the crossroad, similar to 'Grüne Brücke'.

Nevertheless, the $PM_{2.5}$ differences at both sites were not significantly higher than other extrema during the runs. The relative differences varied more strongly among the days than along the study route. A reason for this is that the absolute and relative differences between 1.0 and 1.6 m levels seem to depend on the absolute $PM_{2.5}$ concentrations controlled by the changing weather conditions throughout the measurement campaign (Fig. 5). These results may be significant for health risk analyses of children. Due to their still developing respiratory tract, any given $PM_{2.5}$ concentration leads to higher levels of exposure for children compared to adults (Habre et al., 2014; Nachman and Parker, 2012). Our data show that the absolute $PM_{2.5}$ concentrations at children breathing height were consistently higher than at adult breathing height, independent of the measurement location. This in turn leads to a disproportionately higher exposure of children, and therefore a higher chance to develop respiratory diseases such as asthma, regardless of the particular site of the children in an urban environment (Khreis et al., 2017). However, our study includes only eight measurement runs using low-cost measurement hardware, which is still at a relatively early stage of development when compared to the established and officially used PM measurement technologies. Further research over longer periods and using advanced hardware is needed to improve our understanding of $PM_{2.5}$ exposure differences between children and adults.

### 4.3. Influence of traffic-exhaust emissions on $PM_{2.5}$

The recorded higher $PM_{2.5}$ exposure of children is supported by the microclimate model simulation. Fed with meteorological parameters from 11 to 24 as boundary conditions, the model simulated $PM_{2.5}$ exposure at 4 pm higher at 1.0 than at 1.8 m. These differences were also independent of the location on the route (Fig. 7). The relative differences between children and adult breathing heights are plausible as $PM_{2.5}$ was emitted at 0.2 m height in the model. At least six local maxima of simulated relative differences could be allocated to real-world, recorded maxima, even though the horizontal resolution of the model is only $5 \times 5$ m (Fig. 7). These sites are located nearby streets with high traffic intensities and where the horizontal dispersion of traffic-related particles is limited by high-rising buildings and narrow streets (Fig. 7, dots 1–6).

$PM_{2.5}$ maxima appear related to the low horizontal wind speeds in the simulation combined with the low irradiation due to a closed cloud cover causing lowered thermal convection and, in consequence, low vertical exchange of emitted $PM_{2.5}$. These findings were limited on traffic-related locations. Within areas of lower traffic occurrences, i.e. the middle of the study area (250–1500 m on the route; Fig. 8), the relative differences show little variability. However, the variance of relative differences was also low at the 'Kaiserstraße' featuring a wide road with fewer obstacles supporting the dispersion of emission, resulting in lower concentrations (4700–5250 m on the route). These findings correspond to results of Paas and Schneider (2016) demonstrating that the simulated dispersion of $PM_{10}$ was also underpredicted throughout the study area. It should be noted though that the simulation represents a snapshot of relative differences for a distinct time. Local variabilities of $PM_{2.5}$ pollution (e.g. higher number of busses and trucks or a traffic jam at the certain time of measurement) cannot be represented, so that a reduced variability and fewer maxima were expected. Furthermore, emission sources like tyre and break abrasions as well as whirled up PM2.5 are not simulated, but have a distinct impact on $PM_{2.5}$ (Karagulian et al., 2019; Sharma and Kumar, 2020). On the other hand, the modelled maxima were more pronounced compared to mean $PM_{2.5}$ levels, which could be affected by the larger vertical difference of 0.8 m due to the grid cell size. Nevertheless, all relative differences were >30% lower than the measurements. These underestimated differences could additionally be related to the fact that the model started with a clean atmosphere including no background concentration of particulate matter and only traffic related $PM_{2.5}$ as an emission source. However, the results of the simulation corroborated that $PM_{2.5}$ emitted by vehicle exhausts alone are a cause of the measured relative differences in $PM_{2.5}$ exposure.

## 5. Conclusion

Our results show that the absolute $PM_{2.5}$ exposure at both heights were related to the stability of the prevailing weather condition, particularly to wind speeds. We conclude that in six out of eight measurement runs, children were significantly more exposed to $PM_{2.5}$ than adults, independent of the position along the measurement runs. Relative $PM_{2.5}$ differences ranged from 122% (11-20) to 175% (11-22) among the runs. The absolute and relative height differences were positively correlated with $PM_{2.5}$ concentrations. Relative differences also varied more strongly among days than along the study route, whereby the latter showed a tendency towards lower variability with increasing absolute concentrations. Explanatory approaches include accumulation processes of local, near ground emitters causing higher exposure differences between 1.0 and 1.6 m, when the absolute $PM_{2.5}$ increase. On the other hand, deviations in absolute $PM_{2.5}$ was leveled out in differences due to similar progression at both heights. However, two sites with local $PM_{2.5}$ concentration maxima ('Grüne Brücke', 'Rheinallee') are still visible in absolute and relative differences.

A simulation of traffic-related $PM_{2.5}$ exposure within the study area shows similar results, whereby at least six local maxima of simulated relative differences can be attributed to measured maxima. Height differences in areas with low traffic intensity cannot be displayed by the model, which is why we suggest that other sources including tyre and break abrasion as well as whirled up, play an important role in $PM_{2.5}$ traffic emission.

In general, the study demonstrated that highly time-resolved measurements, and subsequent comparisons, of $PM_{2.5}$ exposure with low-cost OPC-N3 sensors are appropriate after initial calibration during $RH < 85\%$ conditions.

## Funding

## CRediT authorship contribution statement

**Harr Lorenz:** Conceptualization, Methodology, Investigation, Data curation, Visualization, Writing – original draft. **Tim Sinsel:** Data curation, Software, Writing – review & editing. **Helge Simon:** Conceptualization, Software, Writing – review & editing. **Oliver Konter:** Writing – review & editing. **Damian Dreiseitl:** Resources, Software, Investigation, Writing – review & editing. **Philipp Schulz:** Investigation, Writing – review & editing. **Esper Jan:** Conceptualization, Supervision, Writing – review & editing.

## Declaration of Competing Interest

The authors declare that they have no known competing financial interests or personal relationships that could have appeared to influence the work reported in this paper.

## Appendix A. Supplementary data

Supplementary data to this article can be found online at https://doi.org/10.1016/j.uclim.2022.101198.

## References

Alfano, B., Barretta, L., Del Giudice, A., de Vito, S., Di Francia, G., Esposito, E., Formisano, F., Massera, E., Miglietta, M.L., Polichetti, T., 2020. A review of low-cost particulate matter sensors from the developers' perspectives. Sensors (Basel, Switzerland) 20 (23). https://doi.org/10.3390/s20236819.

Alphasense, 2018. Technical Information Release December 2018: Alphasense Particle Counter OPC-N Range Product Update. http://www.alphasense.com/WEB1213/wp-content/uploads/2019/02/OPC-N3-information-update-Dec-18.pdf (Accessed 1 April 2021).

Azarmi, F., Kumar, P., Marsh, D., Fuller, G., 2016. Assessment of the long-term impacts of PM10 and PM2.5 particles from construction works on surrounding areas. Environ Sci Process Impacts 18 (2), 208–221. https://doi.org/10.1039/c5em00549c.

Bohren, C.F., Huffman, D.R., 1998. Absorption and Scattering of Light by Small Particles. Wiley. https://doi.org/10.1002/9783527618156.

Brattich, E., Bracci, A., Zappi, A., Morozzi, P., Di Sabatino, S., Porcù, F., Di Nicola, F., Tositti, L., 2020. How to get the best from low-cost particulate matter sensors: guidelines and practical recommendations. Sensors (Basel, Switzerland) 20 (11). https://doi.org/10.3390/s20113073.

Bruse, M., 1999. Die Auswirkungen kleinskaliger Umweltgestaltung auf das Mikroklima: Entwicklung des prognostischen numerischen Modells ENVI-met zur Simulation der Wind-, Temperatur- und Feuchteverteilung in städtischen Strukturen (Dissertation, Bochum, 217 pp.).

Bulot, Florentin, et al., 2019. Long-term field comparison of multiple low-cost particulate matter sensors in an outdoor urban environment. Sci. Rep. 9 (1) https://doi.org/10.1038/s41598-019-43716-3.

Chatzidiakou, L., Krause, A., Popoola, O.A.M., Di Antonio, A., Kellaway, M., Han, Y., Squires, F.A., Wang, T., Zhang, H., Wang, Q., Fan, Y., Chen, S., Hu, M., Quint, J.K., Barratt, B., Kelly, F.J., Zhu, T., Jones, R.L., 2019. Characterising low-cost sensors in highly portable platforms to quantify personal exposure in diverse environments. Atmospheric Measurement Tech. 12 (8), 4643–4657. https://doi.org/10.5194/amt-12-1-2019.

Cheng, Y.-H., Li, Y.-S., 2010. Influences of traffic emissions and meteorological conditions on ambient PM10 and PM2.5 levels at a highway Toll Station. Aerosol air. Qual. Res. 10 (5), 456–462. https://doi.org/10.4209/aaqr.2010.04.0025.

Crilley, L.R., Shaw, M., Pound, R., Kramer, L.J., Price, R., Young, S., Lewis, A.C., Pope, F.D., 2018. Evaluation of a low-cost optical particle counter (Alphasense OPC-N2) for ambient air monitoring. Atmos. Meas. Tech. 11 (2), 709–720. https://doi.org/10.5194/amt-11-709-2018.

Crilley, L.R., Singh, A., Kramer, L.J., Shaw, M.D., Alam, M.S., Apte, J.S., Bloss, W.J., Hildebrandt Ruiz, L., Fu, P., Fu, W., Gani, S., Gatari, M., Ilyinskaya, E., Lewis, A. C., Ng'ang'a, D., Sun, Y., Whitty, R.C.W., Yue, S., Young, S., Pope, F.D., 2020. Effect of aerosol composition on the performance of low-cost optical particle counter correction factors. Atmos. Meas. Tech. 13 (3), 1181–1193. https://doi.org/10.5194/amt-13-1181-2020.

Czernecki, B., Półrolniczak, M., Kolendowicz, L., Marosz, M., Kendzierski, S., Pilguj, N., 2017. Influence of the atmospheric conditions on PM10 concentrations in Poznań, Poland. J. Atmos. Chem. 74 (1), 115–139. https://doi.org/10.1007/s10874-016-9345-5.

Deutscher Wetterdienst, 2021a. Niederschlag: vieljährige Mittelwerte 1981–2010. Deutscher Wetterdienst. https://www.dwd.de/DE/leistungen/klimadatendeutschland/mittelwerte/nieder_8110_fest_html.html?view=nasPublication&nn=16102 (Accessed 10 May 2021).

Deutscher Wetterdienst, 2021b. Temperatur: vieljährige Mittelwerte 1981–2010. https://www.dwd.de/DE/leistungen/klimadatendeutschland/mittelwerte/temp_8110_fest_html.html%3Fview%3DnasPublication.

Di Antonio, A., Popoola, O.A.M., Ouyang, B., Saffell, J., Jones, R.L., 2018. Developing a relative humidity correction for low-cost sensors measuring ambient particulate matter. Sensors (Basel, Switzerland) 18 (9). https://doi.org/10.3390/s18092790.

Environmental Protection Agency of Germany (UBA), 2017. The Handbook of Emission Factors for Road Transport (HBEFA). https://www2.dmu.dk/AtmosphericEnvironment/Docs/NO2scheme.pdf (Accessed 12.03.21).

Espressif, 2021. ESP32. https://www.espressif.com/en/products/socs/esp32 (Accessed 5 February 2021).

European Parliament and Council (EU), 2008. Directive 2008/50/EC of the European Parliament and of the Council of 21 May 2008 on Ambient Air Quality and Cleaner Air for Europe. https://eur-lex.europa.eu/eli/dir/2008/50/oj.

Feng, S., Gao, D., Liao, F., Zhou, F., Wang, X., 2016. The health effects of ambient PM2.5 and potential mechanisms. Ecotoxicol. Environ. Saf. 128, 67–74. https://doi.org/10.1016/j.ecoenv.2016.01.030.

Fortune, S., 1987. A sweepline algorithm for Voronoi diagrams. Algorithmica 2 (1–4), 153–174. https://doi.org/10.1007/BF01840357.

Gallagher, J., Baldauf, R., Fuller, C.H., Kumar, P., Gill, L.W., McNabola, A., 2015. Passive methods for improving air quality in the built environment: a review of porous and solid barriers. Atmos. Environ. 120, 61–70. https://doi.org/10.1016/j.atmosenv.2015.08.075.

Garcia-Algar, O., Canchucaja, L., d'Orazzio, V., Manich, A., Joya, X., Vall, O., 2015. Different exposure of infants and adults to ultrafine particles in the urban area of Barcelona. Environ. Monit. Assess. 187 (1), 4196. https://doi.org/10.1007/s10661-014-4196-5.

Goel, A., Kumar, P., 2016. Vertical and horizontal variability in airborne nanoparticles and their exposure around signalised traffic intersections. Environ. Pollution (Barking, Essex: 1987) 214, 54–69. https://doi.org/10.1016/j.envpol.2016.03.033.

Goldman, L.R., 1995. Children–unique and vulnerable. Environmental risks facing children and recommendations for response. Environ. Health Perspect. 103 (Suppl. 6), 13–18. https://doi.org/10.1289/ehp.95103s613.

Graham, A.M., Pringle, K.J., Arnold, S.R., Pope, R.J., Vieno, M., Butt, E.W., Conibear, L., Stirling, E.L., McQuaid, J.B., 2020. Impact of weather types on UK ambient particulate matter concentrations. Atmospheric Environment: X 5, 100061. https://doi.org/10.1016/j.aeaoa.2019.100061.

Gualtieri, M., Ovrevik, J., Mollerup, S., Asare, N., Longhin, E., Dahlman, H.-J., Camatini, M., Holme, J.A., 2011. Airborne urban particles (Milan winter-PM2.5) cause mitotic arrest and cell death: effects on DNA, mitochondria, AhR binding and spindle organization. Mutat. Res. 713 (1–2), 18–31. https://doi.org/10.1016/j.mrfmmm.2011.05.011.

Gysel, M., Crosier, J., Topping, D.O., Whitehead, J.D., Bower, K.N., Cubison, M.J., Williams, P.I., Flynn, M.J., McFiggans, G.B., Coe, H., 2007. Closure study between chemical composition and hygroscopic growth of aerosol particles during TORCH2. Atmos. Chem. Phys. 7 (24), 6131–6144. https://doi.org/10.5194/acp-7-6131-2007.

Habre, R., Moshier, E., Castro, W., Nath, A., Grunin, A., Rohr, A., Godbold, J., Schachter, N., Kattan, M., Coull, B., Koutrakis, P., 2014. The effects of PM2.5 and its components from indoor and outdoor sources on cough and wheeze symptoms in asthmatic children. J. Exposure Sci. Environ. Epidemiol. 24 (4), 380–387. https://doi.org/10.1038/jes.2014.21.

Hagler, G.S.W., Williams, R., Papapostolou, V., Polidori, A., 2018. Air quality sensors and data adjustment algorithms: when is it no longer a measurement? Environ. Sci. Technol. 52 (10), 5530–5531. https://doi.org/10.1021/acs.est.8b01826.

Hamburger, T., McMeeking, G., Minikin, A., Birmili, W., Dall'Osto, M., O'Dowd, C., Flentje, H., Henzing, B., Junninen, H., Kristensson, A., de Leeuw, G., Stohl, A., Burkhart, J.F., Coe, H., Krejci, R., Petzold, A., 2011. Overview of the synoptic and pollution situation over Europe during the EUCAARI-LONGREX field campaign. Atmos. Chem. Phys. 11 (3), 1065–1082. https://doi.org/10.5194/acp-11-1065-2011.

Hoffmann, J., 2019. DWD. SXEU31 DWAV 200800. Synoptische Übersicht Kurzfrist. https://www.wetterzentrale.de/article.php?id=70603&lang=1.

Imhof, D., Weingartner, E., Vogt, U., Dreiseidler, A., Rosenbohm, E., Scheer, V., Vogt, R., Nielsen, O.J., Kurtenbach, R., Corsmeier, U., Kohler, M., Baltensperger, U., 2005. Vertical distribution of aerosol particles and NOx close to a motorway. Atmos. Environ. 39 (31), 5710–5721. https://doi.org/10.1016/j.atmosenv.2004.07.036.

Karagulian, F., Belis, C.A., Dora, C.F.C., Prüss-Ustün, A.M., Bonjour, S., Adair-Rohani, H., Amann, M., 2015. Contributions to cities' ambient particulate matter (PM): a systematic review of local source contributions at global level. Atmos. Environ. 120, 475–483. https://doi.org/10.1016/j.atmosenv.2015.08.087.

Karagulian, F., Barbiere, M., Kotsev, A., Spinelle, L., Gerboles, M., Lagler, F., Redon, N., Crunaire, S., Borowiak, A., 2019. Review of the performance of low-cost sensors for air quality monitoring. Atmosphere 10 (9), 506. https://doi.org/10.3390/atmos10090506.

Khreis, Haneen, et al., 2017. Exposure to traffic-related air pollution and risk of development of childhood asthma: A systematic review and meta-analysis. Environ. Int. https://doi.org/10.1016/j.envint.2016.11.012.

Kumar, P., Fennell, P., Britter, R., 2008. Measurements of particles in the 5–1000 nm range close to road level in an urban street canyon. Sci. Total Environ. 390 (2–3), 437–447. https://doi.org/10.1016/j.scitotenv.2007.10.013.

Kumar, P., Khare, M., Harrison, R.M., Bloss, W.J., Lewis, A.C., Coe, H., Morawska, L., 2015. New directions: air pollution challenges for developing megacities like Delhi. Atmos. Environ. 122, 657–661. https://doi.org/10.1016/j.atmosenv.2015.10.032.

Kumar, P., Rivas, I., Sachdeva, L., 2017. Exposure of in-pram babies to airborne particles during morning drop-in and afternoon pick-up of school children. Environ. Pollution (Barking, Essex: 1987) 224, 407–420. https://doi.org/10.1016/j.envpol.2017.02.021.

Lelieveld, J., Klingmüller, K., Pozzer, A., Pöschl, U., Fnais, M., Daiber, A., Münzel, T., 2019. Cardiovascular disease burden from ambient air pollution in Europe reassessed using novel hazard ratio functions. Eur. Heart J. 40 (20), 1590–1596. https://doi.org/10.1093/eurheartj/ehz135.

Mazur, L.J., 2003. Pediatric environmental health. Curr. Problems Pediatric Adolescent Health Care 33 (1), 6–25. https://doi.org/10.1067/mps.2003.1.

McCauley, J.D., Aime, A., Blazek, R., Metz, M., 2020. GRASS GIS 7.9.dev Reference Manual: v.voronoi. https://grass.osgeo.org/grass79/manuals/v.voronoi.html.

McGregor, G.R., Bamzelis, D., 1995. Synoptic typing and its application to the investigation of weather air pollution relationships, Birmingham, United Kingdom. Theor. Appl. Climatol. 51 (4), 223–236. https://doi.org/10.1007/BF00867281.

Mie, G., 1908. Beiträge zur Optik trüber Medien, speziell kolloidaler Metallösungen. Ann. Phys. 330 (3), 377–445. https://doi.org/10.1002/ANDP.19083300302.

Morawska, Lidia, et al., 2018. Applications of low-cost sensing technologies for air quality monitoring and exposure assessment: How far have they gone? Environ. Int. 116, 286–299. https://doi.org/10.1016/j.envint.2018.04.018.

Nachman, K.E., Parker, J.D., 2012. Exposures to fine particulate air pollution and respiratory outcomes in adults using two national datasets: a cross-sectional study. Environ. Health 11, 25. https://doi.org/10.1186/1476-069X-11-25.

Paas, B., Schneider, C., 2016. A comparison of model performance between ENVI-met and Austal2000 for particulate matter. Atmos. Environ. 145, 392–404. https://doi.org/10.1016/j.atmosenv.2016.09.031.

Petters, M.D., Kreidenweis, S.M., 2007. A single parameter representation of hygroscopic growth and cloud condensation nucleus activity. Atmos. Chem. Phys. 7 (8), 1961–1971. https://doi.org/10.5194/acp-7-1961-2007.

Sharma, A., Kumar, P., 2020. Quantification of air pollution exposure to in-pram babies and mitigation strategies. Environ. Int. 139, 105671 https://doi.org/10.1016/j.envint.2020.105671.

Shepard, D., 1968. A two-dimensional interpolation function for irregularly-spaced data. In: Proceedings of the 1968 23rd ACM National Conference on -. the 1968 23rd ACM National Conference, Not Known. ACM Press, New York, New York, USA, pp. 517–524. https://doi.org/10.1145/800186.810616.

Simcom, 2021. Sim28. https://www.simcom.com/product/SIM28.html (Accessed 5 February 2021).

Simon, H., Fallmann, J., Kropp, T., Tost, H., Bruse, M., 2019. Urban trees and their impact on local ozone concentration—a microclimate modeling study. Atmosphere 10 (3), 154. https://doi.org/10.3390/atmos10030154.

Singh, R.B., Huber, A.H., Braddock, J.N., 2003. Development of a microscale emission factor model for particulate matter for predicting real-time motor vehicle emissions. J. Air Waste Manag. Assoc. (1995) 53 (10), 1204–1217. https://doi.org/10.1080/10473289.2003.10466288.

Sousan, Sinan, Koehler, Kirsten, Hallett, Laura, Peters, Thomas, 2016. Evaluation of the Alphasense optical particle counter (OPC-N2) and the Grimm portable aerosol spectrometer (PAS-1.108). Aerosol Sci. Technol. 50 (12), 1352–1365. https://doi.org/10.1080/02786826.2016.1232859.

Stewart, I.D., Oke, T.R., 2012. Local climate zones for urban temperature studies. Bull. Am. Meteorol. Soc. 93 (12), 1879–1900. https://doi.org/10.1175/BAMS-D-11-00019.1.

Tang, G., Zhang, J., Zhu, X., Song, T., Münkel, C., Hu, B., Schäfer, K., Liu, Z., Zhang, J., Wang, L., Xin, J., Suppan, P., Wang, Y., 2016. Mixing layer height and its implications for air pollution over Beijing, China. Atmos. Chem. Phys. 16 (4), 2459–2475. https://doi.org/10.5194/acp-16-2459-2016.

Torres-Ramos, Y.D., Montoya-Estrada, A., Guzman-Grenfell, A.M., Mancilla-Ramirez, J., Cardenas-Gonzalez, B., Blanco-Jimenez, S., Sepulveda-Sanchez, J.D., Ramirez-Venegas, A., Hicks, J.J., 2011. Urban PM2.5 induces ROS generation and RBC damage in COPD patients. Front. Biosci. (Elite edition) 3, 808–817. https://doi.org/10.2741/e288.

Umweltmeteorologie RLP, 2019. State Office of Rhineland-Palatinate. https://luft.rlp.de/de/umweltmeteorologie/.

Wagner, P., Schäfer, K., 2017. Influence of mixing layer height on air pollutant concentrations in an urban street canyon. Urban Clim. 22, 64–79. https://doi.org/10.1016/j.uclim.2015.11.001.

Walser, A., Sauer, D., Spanu, A., Gasteiger, J., Weinzierl, B., 2017. On the parametrization of optical particle counter response including instrument-induced broadening of size spectra and a self-consistent evaluation of calibration measurements. Atmos. Meas. Tech. 10 (11), 4341–4361. https://doi.org/10.5194/amt-10-4341-2017.

Wania, A., Bruse, M., Blond, N., Weber, C., 2012. Analysing the influence of different street vegetation on traffic-induced particle dispersion using microscale simulations. J. Environ. Manag. 94 (1), 91–101. https://doi.org/10.1016/j.jenvman.2011.06.036.

Wickham, H., 2020. Package 'plyr': Tools for Splitting, Applying and Combining Data; Version 1.8.6. http://had.co.nz/plyr (Accessed 10.02.21).

Zauli Sajani, S., Marchesi, S., Trentini, A., Bacco, D., Zigola, C., Rovelli, S., Ricciardelli, I., Maccone, C., Lauriola, P., Cavallo, D.M., Poluzzi, V., Cattaneo, A., Harrison, R.M., 2018. Vertical variation of PM2.5 mass and chemical composition, particle size distribution, NO2, and BTEX at a high rise building. Environ. Pollution (Barking, Essex: 1987) 235, 339–349. https://doi.org/10.1016/j.envpol.2017.12.090.

Zeuschner, J., 2019. DWD. SXEU31 DWAV 230800. Synoptische Übersicht Kurzfrist. https://www.wetterzentrale.de/article.php?id=70739&lang=1.

Zhou, S., Wu, L., Guo, J., Chen, W., Wang, X., Zhao, J., Cheng, Y., Huang, Z., Zhang, J., Sun, Y., Fu, P., Jia, S., Chen, Y., Kuang, J., 2019. Vertical Distribution of Atmospheric Particulate Matters within Urban Boundary Layer in Southern China: Size-segregated Chemical Composition and Secondary Formation through Cloud Processing and Heterogeneous Reactions. https://doi.org/10.5194/acp-2019-155.

ZIMEN, 2019. Luft-Überwachung in Rheinland-Pfalz. State Office of Rhineland-Palatinate. https://luft.rlp.de/de/startseite/.